Available online at www.sciencedirect.com
SCIENCE DIRECT®
Engineering Structures 25 (2003) 993–1007
ENGINEERING STRUCTURES
www.elsevier.com/locate/engstruct

Computational model for post cracking analysis of RC membrane elements based on local stress–strain characteristics

Masoud Soltani [a,*], Xuehui An [b], Koichi Maekawa [a]

[a] Department of Civil Engineering, The University of Tokyo, Hongo 7-3-1, Bunkyo-ku, Tokyo 113, Japan
[b] Department of Hydraulic Engineering, Tsinghua University, Beijing 100084, China

Received 4 March 2002; received in revised form 28 January 2003; accepted 30 January 2003

Abstract

This paper aims at the development of a computational model for analysis of RC membrane elements subjected to general in-plane stresses. The response of RC elements is computed based on the local stress transfer mechanism in RC domain involving interaction of concrete-reinforcing bars, stress transfer across cracks due to aggregate interlock and dowel action with consideration to the kinking effect of reinforcements at the crack plane. Using the proposed method, the spatial average stress-strain relationship of reinforcing bars and cracked concrete, both normal and along the crack plane, and the average crack spacing and crack width are computed. Verification of the method is carried out through comparison with some experiment results.

Keywords: Tension stiffening; RC; Membrane element; Bond; Crack spacing; Crack width; Aggregate interlock

1. Introduction

RC membrane elements are basic components of many RC structures, such as shear walls, offshore platforms, box girders, shells and folded plates. The fundamental behavior of RC membrane elements is complex due to significant contributions of different mechanisms, such as concrete-reinforcing bar interaction, aggregate interlock, dowel action, bridging stress and reduction of compressive strength after cracking. Due to the complexity of the load transfer mechanism in reinforced concrete elements, many simplifications or neglect of effects can be found in previously developed constitutive models [1–3]. The average stress–strain relationship of reinforcing bars and concrete used in previously developed theories (smeared crack models) has usually been derived based on uniaxial direct tension tests, that do not actually coincide with the experimental results on RC panels [4,5]. Cracks generated in RC membrane elements may have any arbitrary inclinations to reinforcing bars. In such cases, the crack spacing is different compared to the direct tension test and also average tensile strain of cracked concrete is different from the reinforcing bars, as a result the mean response of concrete and reinforcing bars differs from the uniaxial direct tension case.

The cracking response and spatial average behavior of reinforced concrete in tension, in which, cracks form perpendicular to the reinforcements, have widely been investigated during the past. However, little effort has been made to investigate the effect of crack and reinforcement inclinations on the post cracking constitutive models of RC elements. Pang and Hsu [5] in development of the so called ‘Softened Truss Model’, experimentally showed that the mean yield strength of reinforcing bars embedded in RC elements under pure shear (cracks in 45 degrees) is less than direct tension, and concluded that this effect is due to the local kinking of steel bars at the crack location. Hauke and Maekawa [4] developed a second order interpolation method for computing mean strength of the reinforcing bars and tension stiffening of concrete with respect to crack inclination. For the case of crack normal to the reinforcing bars, the tension stiffening and mean strength of reinforcements, derived in direct tension, are considered and for cracks parallel to the reinforcements, tension

* Corresponding author. Fax: +81-3-5841-6010.
E-mail address: masouds@concrete.t.u-tokyo.ac.jp (M. Soltani).

0141-0296/03/$ - see front matter © 2003 Elsevier Science Ltd. All rights reserved.
doi:10.1016/S0141-0296(03)00042-7

Nomenclature

A_s, I_s area and moment of inertia of bar section;
d diameter of reinforcing bar;
e, e_{max} normalized compressive strain and its maximum value;
e_p, k equivalent plastic strain and fracture parameter;
E_s elastic modulus of bar section;
$f_{crX'}$, $f_{crY'}$ axial steel stresses at crack location;
$f_d(x)$ shear stress of re-bar due to bending curvature;
$f_{dX'}$, $f_{dY'}$ shear stresses of reinforcing bars at the crack location;
$f_{d\theta}$ tensile stress induced by shear stress in steel bar;
$f_{mid\text{-}X'}$, $f_{mid\text{-}Y'}$ local steel stresses at the midline between two adjacent cracks;
f_t, f'_c tensile strength and cylindrical compressive strength of concrete;
$f_{X'}$,$f_{Y'}$ average axial stresses of reinforcing bars;
f_y, f'_y yield strength and reduced mean yield stress of steel bar;
$g(\varepsilon_s)$ strain reduction function in bond-slip model;
G_f fracture energy of plain concrete;
K foundation stiffness of concrete;
L_b, L_c bond deterioration and curvature influencing length;
L_{c0} curvature influencing length in the elastic range;
L_e, $L_{eX'}$, $L_{eY'}$ length of reinforcing bars between two adjacent cracks;
$M(x)$, $V(x)$ bending moment and shear force along the bar axis;
N_{cr} number of generated cracks;
s non-dimensional slip;
S local slip along reinforcing bar;
S_0, S_{XY} initial and average crack spacing;
x distance from the middle of re-bars between adjacent cracks;
y local coordinate of steel fiber from center of bar section;
α inclination of reinforcement;
β angle between reinforcement and crack;
δ_b half deflection of the reinforcing bar;
δ_s, $\delta_{sX'}$, $\delta_{sY'}$ deflections of reinforcing bars;
ε_c compressive strain correspond to peak stress;
ε_f, σ_f fiber strain and stress of bar cross section;
ε_s,σ_s local strain and stress of steel bar;
$\bar{\varepsilon}_s$,$\bar{\sigma}_s$ average strain and stress of steel bar;
ε_X, ε_Y, γ_{XY} normal strains (ε) and shear strain (γ) of element in global directions (X–Y);
$\varepsilon_{X'}$, $\varepsilon_{Y'}$, $\gamma_{X'Y'}$ normal and shear strains of re-bars in local coordinate system (X'–Y');
ε_1, ε_2, γ_{12} normal and shear strains of concrete in local coordinate system (1–2);
$\phi(x)$,ϕ_{max} curvature of reinforcing bar and its maximum value;
μ non-dimensional damage parameter;
θ inclination of normal to crack with respect to X direction;
$\rho_{X'}$,$\rho_{Y'}$ reinforcement ratios in X' and Y' directions;
σ_{br},σ_d bridging and dilatancy stresses transfer across crack;
$\sigma_{C.L.}$ local concrete stress at midline between two adjacent cracks;
σ_t tensile stress developed in concrete due to bond and shear stresses of steel bars;
σ_X, σ_Y, τ_{XY} normal stresses (σ) and shear stress (τ) of element in global directions (X–Y);
σ_1, σ_2,τ_{12} normal and shear stresses of concrete in local coordinate system (1–2);
$\tau(\varepsilon_s s)$, τ local bond stress;
$\bar{\tau}$ average bond stress along a small segment;
τ_{agg}, τ_{st} shear stress transfer by aggregate interlock and reinforcing bars;
$\tau_0(s)$ intrinsic bond stress for strain equal to zero;
ω,δ opening and shear slipping of crack;
ψ shear slip to crack opening ratio;
ζ reduction factor for fracture parameter.

softening and a bare bar model can be adopted. So, for any other inclination they proposed the interpolation between these two behaviors.

The stress transfer ability of the cracked concrete in RC element involving tension stiffening and shear stress across crack strictly affects the cracking response, failure mode and capacity of RC elements that can be evaluated if the cracking behavior and stress transfer mechanism of these elements are understood well. Local stress analysis considering local deformations (crack opening and slip) and bond performance between concrete and reinforcement has recently been noted as an advanced numerical tool for future study of the structural behavior of reinforced concrete [6,7].

The computational method described herein is an attempt at formulating post cracking response of reinforced concrete membrane elements in terms of stresses at the crack faces, taking into account all characteristics of stress transferring in RC elements (Fig. 1). The local stress-strain characteristics of concrete and reinforcing bars embedded in concrete, used in this work, are based on the extensive research activities that during past decades have been undertaken at the University of Tokyo to investigate the fundamental mechanism of local stresses transfer in RC domain (Fig. 1). Using the proposed method, the spatial average behavior of both concrete and reinforcing bars during the crack propagation and stabilizing of cracks can be investigated.

For clarifying the versatility of the proposed method, the systematic verification is carried out through comparison with some experimental results. The parametric study and outline of the method for developing rational constitutive models, considering non-isotropic arrangement of reinforcing bars and bond performance, will be reported in a separate paper.

2. Definitions and assumptions

Fig. 2 shows the state of stresses of a reinforced concrete element subjected to general in-plane stresses in Cartesian coordinate system X–Y. The RC element is orthogonally reinforced with reinforcing bars in X′ and Y′ directions placed at an angle α to the global coordinate system. The principal direction of these applied stresses is defined by 1–2 coordinate system (at angle θ with respect to X direction). The crack direction is initially considered normal to principal direction of tensile stress. The reinforcement ratio in X′ and Y′ direction are defined as $\rho_{X'}$ and $\rho_{Y'}$, respectively.

The following general assumptions are also made:

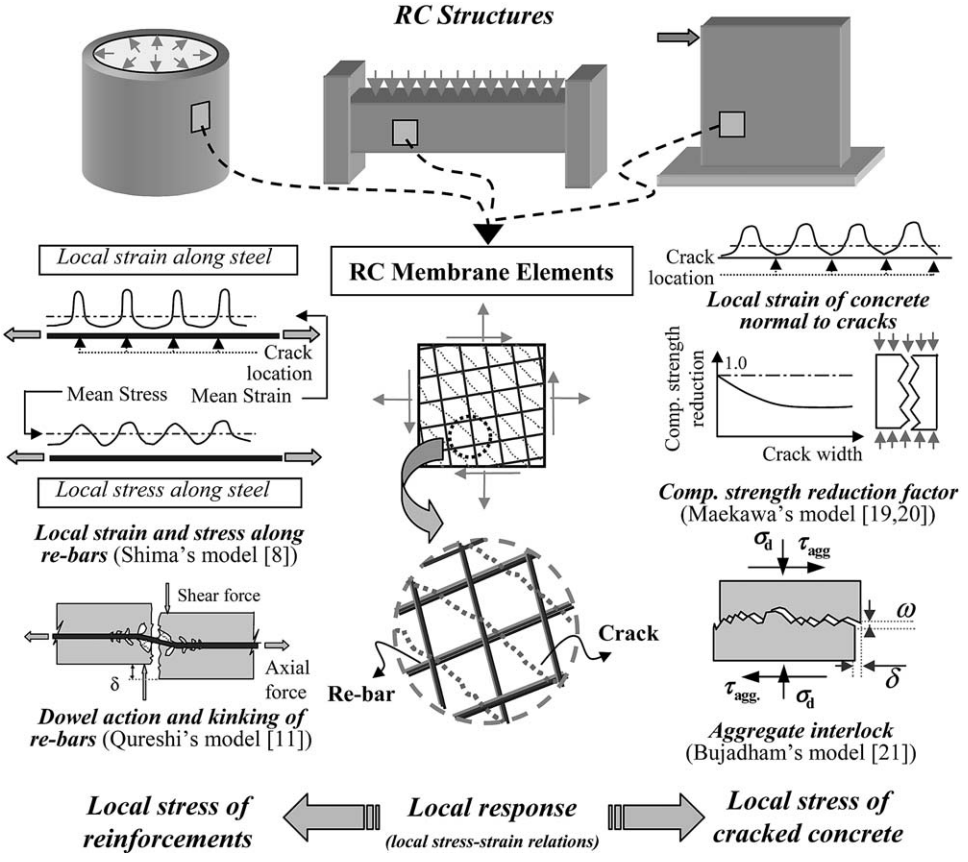

Fig. 1. Local stress transfer mechanism in RC membrane elements.

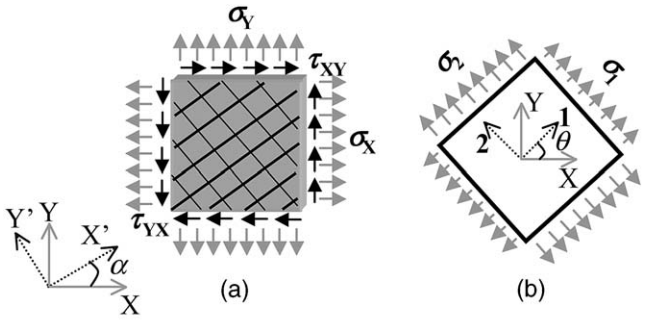

Fig. 2. RC Element subjected to in-plane stresses. (a) applied stresses; (b) principal directions of applied stresses.

- Reinforcing bars placed in uniform and smeared configurations.
- Cracks form in uniform manner and the direction of cracks remain fixed during loading.
- Loads are monotonically applied in terms of normal and shear stresses (σ_X, σ_Y, τ_{XY}).

3. Internal stresses in cracked RC elements

Upon cracking, the smeared steel stresses are activated. Using the equilibrium and compatibility equations, the applied stresses and strains in X–Y coordinate system can be expressed based on those of local coordinate systems of concrete (1–2) and reinforcing bars (X′–Y′) and vice versa.

The state of stresses of concrete and reinforcing bars can be presented based on the average stresses of elements or local stresses at the crack location (Fig. 3). At a distinct cracked section, the local force normal to crack is carried by reinforcing bars and the bridging stress of cracked concrete. The local shear stress along the crack plane is carried by aggregate interlock and dowel action of reinforcing bars. Due to interlocking of aggregates at crack surface, the compression stress, so called 'dilatancy stress', is applied normal to the crack surface (Fig. 3b). The force developing in reinforcing bars is partly transferred to the concrete between adjacent cracks through bond stress between reinforcing bars and concrete, while the bridging stress and stresses due to aggregate interlock (crack dilatancy and shear stress) and dowel action at crack location are directly applied to the fracturing planes.

4. Local stress transfer mechanism along the reinforcing bars

4.1. Bond stress along the reinforcing bars

Owing to bond between concrete and reinforcing bars, some parts of the tensile force are carried by concrete

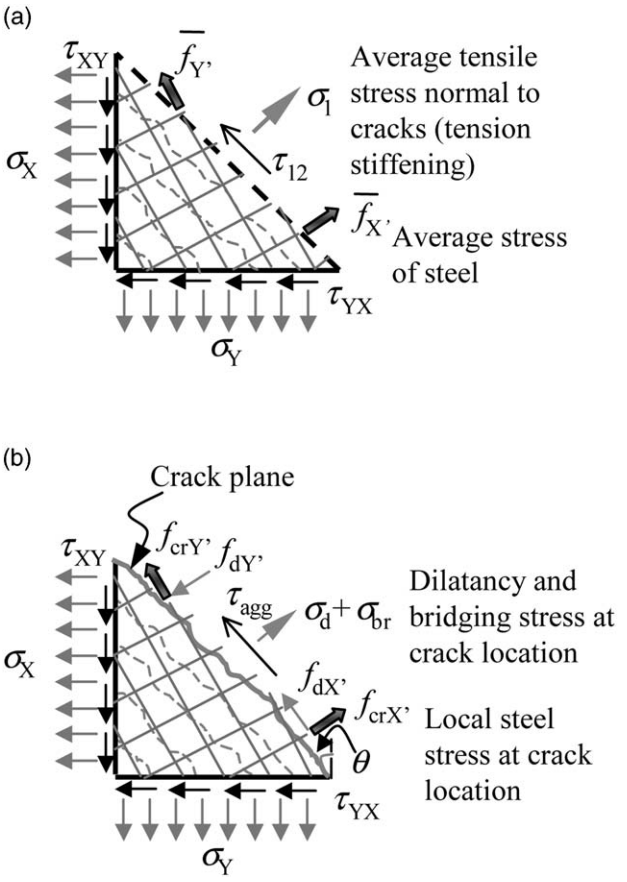

Fig. 3. State of stress of cracked concrete and reinforcing bars. (a) average stresses; (b) local stresses at crack location.

between adjacent cracks. Therefore, the stress-strain relationship of reinforcing bars, on average, is consequently different from bare bar behavior. Steel at the crack location starts to yield before other points along its axis, and as a result, after yielding of re-bar at crack plane, shows lower average stress compared to bare bar. After yielding of reinforcement, some areas close to cracks come into the hardening zone, while the remaining parts are still in the elastic zone. In the present paper, the universal bond-slip-strain model proposed by Shima et al. [8], which is applicable for both elastic and post-yield range, is used. The effect of elasticity, hardening strain and the stiffness in strain hardening zone, in other words the strain-stress characteristics of bare bar, is considered in this model. The local bond stress $\tau(\varepsilon_s,s)$ is expressed as:

$$\tau(\varepsilon_s,s) = \tau_0(s)\, g(\varepsilon_s) \tag{1}$$

$$\tau_0(s) = 0.73 f'_c [\ln(1 + 5s)]^3 \tag{2}$$

$$g(\varepsilon_s) = \frac{1}{1 + 10^5 \varepsilon_s} \tag{3}$$

where, $\tau_0(s)$ is intrinsic bond stress when strain is zero, f'_c is compressive strength of concrete, d and ε_s are diameter and steel strain respectively, s is non-dimen-

sional slip equal to $1000S/d$, S is slip which is computed by integrating the strain over the length of re-bar starting from midway between adjacent cracks (Fig. 4).

The strain function $g(\varepsilon_s)$ controls reduction of bond stress in the post yield range. When the reinforcing bar, starts to yield in vicinity of crack planes, the steel strain suddenly increases to the strain-hardening zone, leading to drop of the local bond stress in plastic region as shown in Fig. 4.

4.2. Bond deterioration zone

The original bond-slip-strain model proposed by Shima et al. [8] has been developed based on tests that were carried out with consideration to an un-bonded zone placed near the loading points. However, in reality, the bond performance near the interface may easily deteriorate due to splitting and crushing of concrete around the bar [9,10].

In order to consider this effect, the 'Bond Deterioration Zone' is considered beside the crack surface (L_b), as defined by Qureshi and Maekawa [11], which is a function of bar diameter (d). Bond stress is assumed to linearly decrease to zero at a distance L_b from the crack surface, and drops to zero at a distance $L_b/2$ from the crack surface (Fig. 5). Based on works of Shin [12], Qureshi and Maekawa [11] the bond deterioration zone can be considered as $5d$ from the crack surface (but not less than the 'Curvature Influencing Zone' as described later).

4.3. Zone of curvature influence

The reinforcing bars under coupled axial load and transverse displacement are bent in the vicinity of cracks. Due to localization of curvature in the reinforcement close to the crack plane, the axial stiffness and the

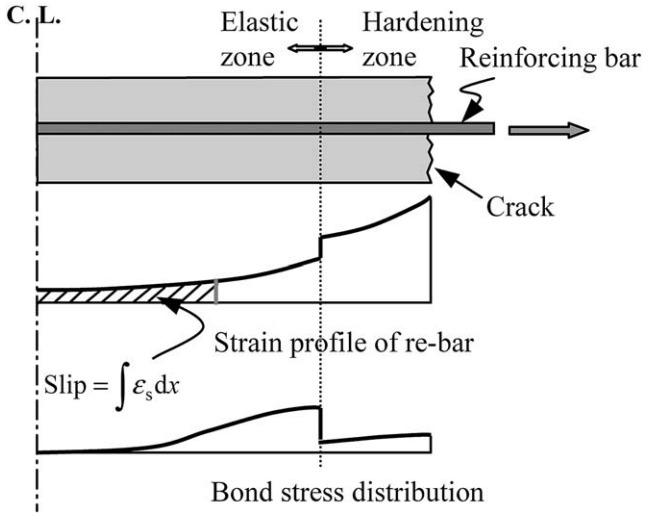

Fig. 4. Bond stress distribution and definition of slip.

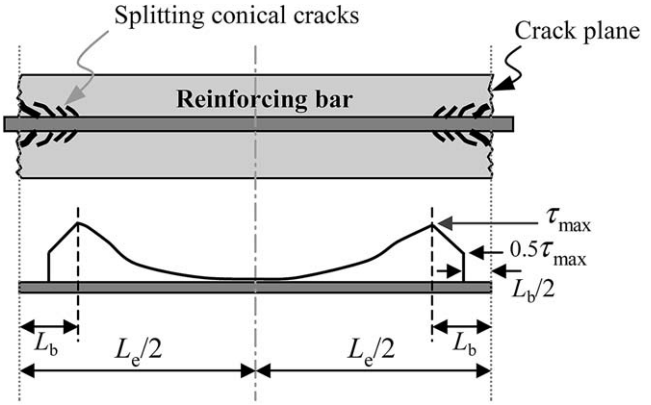

Fig. 5. Bond deterioration beside the crack surface.

mean yield strength of the reinforcements is reduced. In order to consider this effect, the 'Curvature Influencing Zone' close to crack surface (L_c) is considered (Fig. 6). Based on the experiments conducted by Qureshi [10], the curvature-influencing zone was observed to be between $4d$ and $5d$ initially with a small increase in large displacements. In small displacement when both the reinforcing bar and concrete are in the elastic range, the size of curvature zone can be derived from modeling of bar as a beam resting on an elastic foundation [13,11] as:

$$L_{c0} = \frac{3\pi}{4}\sqrt[4]{\frac{4E_sI_s}{Kd}},\quad K = \frac{150f_c'^{0.85}}{d}\ (\text{Unit:}\frac{\text{MPa}}{\text{mm}}) \tag{4}$$

where, K is foundation stiffness for concrete and I_s and E_s are the moment of inertia and elastic modulus of bar section, respectively.

In large deflection, the reinforcing bar and supporting concrete show non-linear behavior and consequently the curvature zone increases. Qureshi and Maekawa [11] considered this effect by proposing an empirical non-dimensional damage parameter as:

$$\mu = (1 + 150\frac{S}{d})\frac{\delta_b}{d} \tag{5}$$

where, S is the axial steel slip and δ_b is equal to half

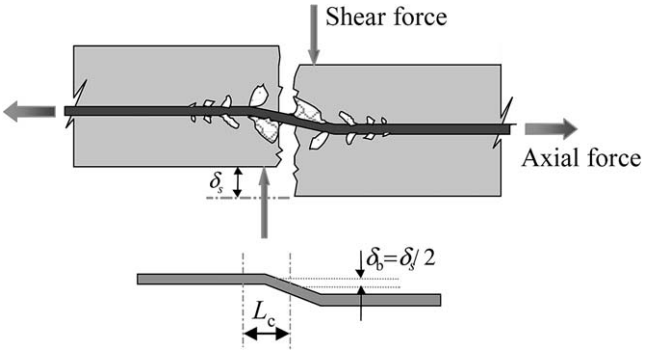

Fig. 6. Curvature of re-bar at the crack surface.

deflection of the reinforcing bar at the interface. Finally the curvature zone is expressed as:

$$L_c = L_{c0} \qquad \mu \le 0.02$$
$$L_c = L_{c0}[1 + 3(\mu - 0.02)^{0.85}] \quad \mu > 0.02. \tag{6}$$

When the reinforcement is oblique to shear plane and pushing against the less confined free surface of the supporting concrete, due to flaking of concrete, both deterioration and curvature zone increase, and as a result shows smaller shear capacity for embedded bar [10,13–15]. This has been shown when the dowel bar pushes against a less confined surface, the curvature zone increases up to $10d$ at a very large angle (close to 180 degrees) between reinforcing bar and crack plane [10] (sign convenience is shown in Fig. 7). In the computation for such a case, the linear interpolation is adopted as:

$$L_c = \text{Original curvature zone}\left(\frac{2\beta}{\pi}\right) \tag{7}$$

where, β is the angle between reinforcement and crack direction. In the case of pushing the bar at right angles to shear plane (Fig. 7b), the original curvature zone (Eq. (6)) can be adopted [10,14].

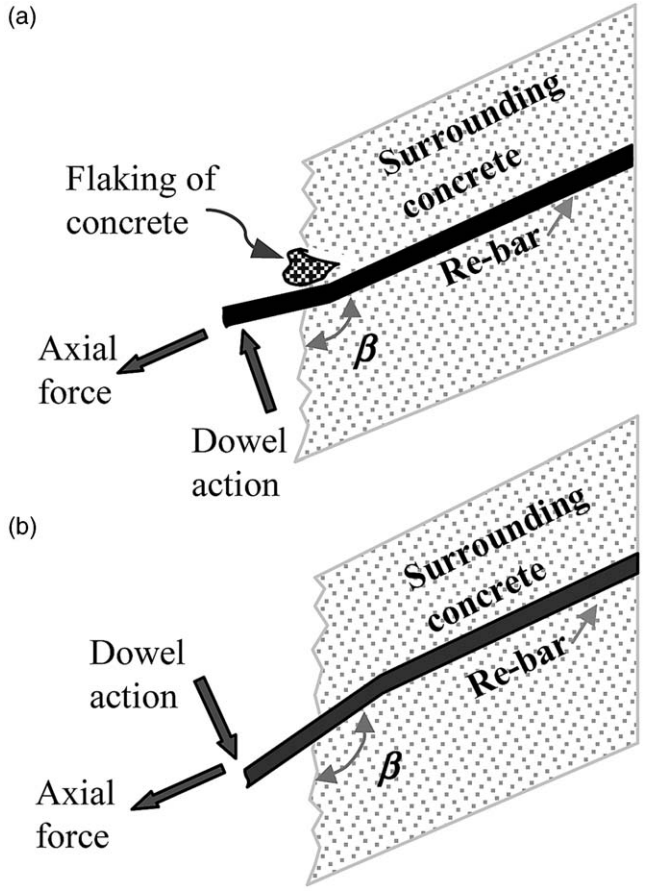

Fig. 7. Curvature influencing zone in the case of reinforcing bar oblique to the cracks. (a) re-bar push less confined surface; (b) re-bar push at right angle to the crack plane.

Considering x as the axis of reinforcing bar, the shape of curvature distribution $\phi(x)$, within L_c can be mathematically modeled by a skew parabolic form [10] as:

$$\phi(x) = \frac{3\phi_{max}}{L_c^2}\left[x - \left(\frac{L_e}{2} - L_c\right)\right]^2, \quad \frac{L_e}{2} - L_c \le x < \frac{L_e}{2} - \frac{L_c}{2}$$
$$\phi(x) = \frac{-3\phi_{max}}{L_c^2}\left[3\left\{x - \left(\frac{L_e}{2} - \frac{L_c}{2}\right)\right\}^2 - L_c\left\{x - \left(\frac{L_e}{2} - \frac{3L_c}{4}\right)\right\}\right],$$
$$\frac{L_e}{2} - \frac{L_c}{2} \le x \le \frac{L_e}{2}. \tag{8}$$

It also coincides well with computed curvature shape based on BEF analogy [10,13]. In Eq. (8) L_e is the length of reinforcing bar between two adjacent cracks and x is considered from the middle of this length. The maximum curvature (ϕ_{max}) is calculated to satisfy the compatibility condition as:

$$\delta_b = \int\int_{\frac{L_e}{2}} \phi(x)dx. \tag{9}$$

4.4. Stress and strain profile along the reinforcing bars

For any given average re-bar strain and length of reinforcing bar between adjacent cracks, the profile of strain and stress along the reinforcement can be computed based on the bond stress distribution along the reinforcing bar.

Satisfying the equilibrium conditions on a small segment along the reinforcing bar, the following equilibrium equation is derived (Fig. 8):

$$\frac{d\sigma_s}{dx} = \frac{\pi d}{A_s}\bar{\tau} \tag{10}$$

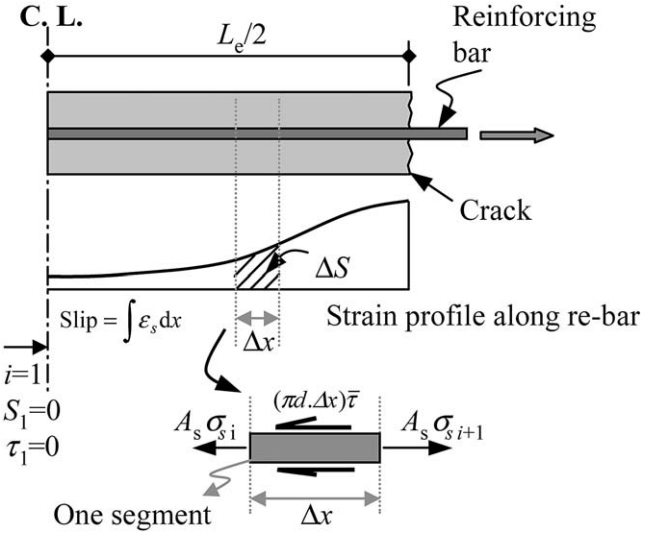

Fig. 8. Equilibrium equation along the small segment.

where, $d\sigma_s/dx$ is gradient of steel stress along the bar, d and A_s are diameter and cross section area of reinforcing bar respectively and $\bar{\tau}$ is the average bond stress along the segment.

The bond stress and the slip at the midway between two adjacent cracks are zero, which are the boundary conditions for the first finite segment. Assuming strain value at the middle of two cracks, the stress and strain profiles are computed by solving the equilibrium and slip compatibility equations, segment by segment along the re-bar.

The flow chart for solving bond-governing equations along the reinforcement is shown in Fig. 9. Starting from the first segment at midway between two adjacent cracks and assuming the strain increment, the stress and the slip value at the other side of the segment and consequently the bond stress, are computed. Increasing the strain increment (compared to the previous step), an iterative procedure is used until the obtained stress value satisfies the equilibrium condition (Eq. (10)). The computed strain and slip for the first segment will be the boundary condition for the next segment. A similar computation procedure follows to attain the stress and strain profile along the reinforcing bar.

In the vicinity of cracks due to curvature, the strains along the bar cross section are not uniform. The strain and stress at the outer fibers of bar cross section are different from the inner fibers. Based on assumed distribution profiles of bond stress and curvature along the curvature zone (Eq. (8)), the sectional averaged mean stress and strain along this region can be computed. The strain for each fiber of cross section is computed as:

$$\varepsilon_f = \varepsilon_s(x) + \phi(x)y \tag{11}$$

where, y is the local coordinate of steel fiber that is measured from the center of the bar cross section, $\varepsilon_s(x)$ is the averaged tensile strain of the section and ε_f is the fiber strain of reinforcing bar. For any fiber strain, the stresses are obtained from the uniaxial stress–strain relationship of bare steel bar. Averaging the fiber stress along the section concerned, the average tensile stress of the section is computed:

$$\sigma_s(x) = \left[\int_{-d/2}^{d/2} \sigma_f(\varepsilon_f)\mathrm{d}A_s(y)\right]/A_s. \tag{12}$$

The computed average tensile strain of each cross section in the curvature influencing zone should satisfy the stress equilibrium along the steel bar (Eq. (10)). The internal cross section force, including the bending

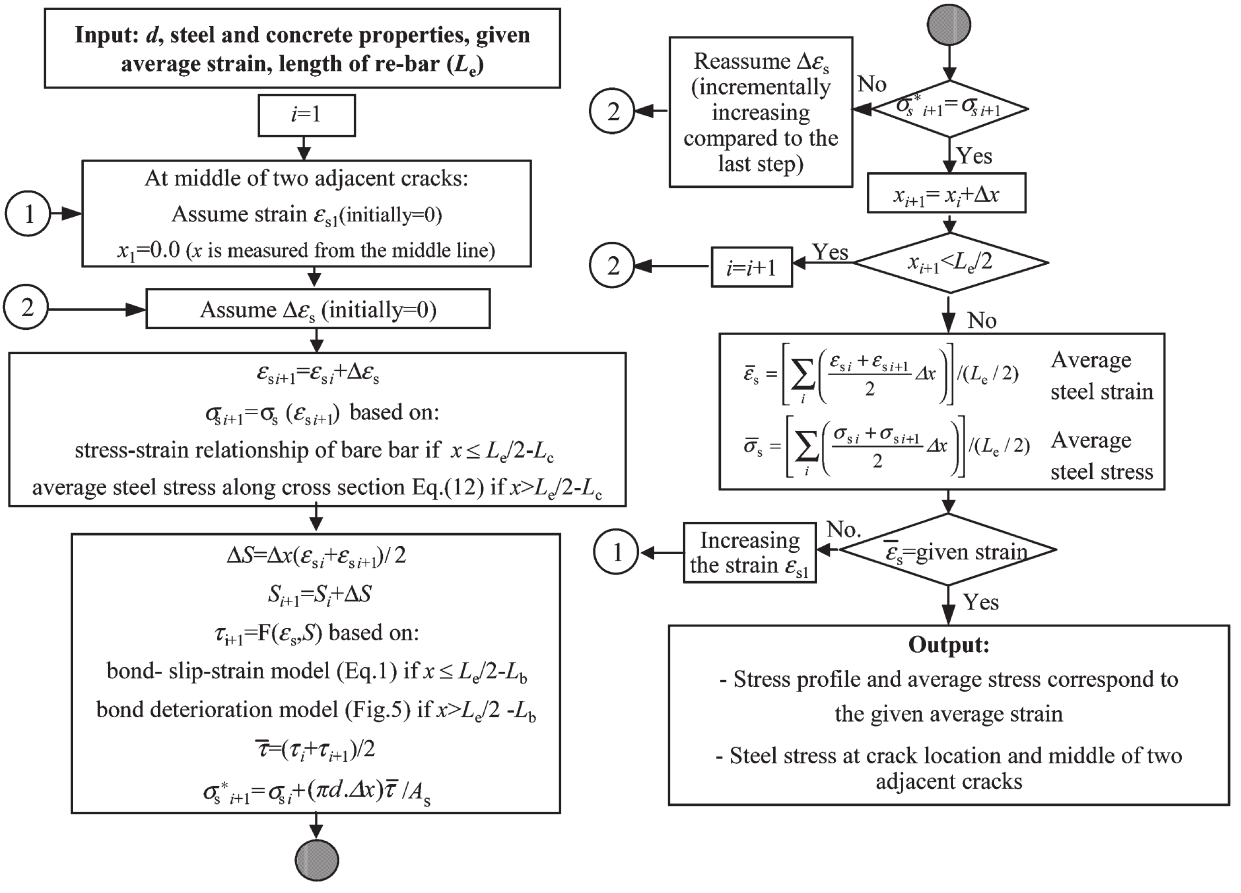

Fig. 9. Flowchart of computing stress-strain profile along the re-bars.

moment $M(x)$ and shear force $V(x)$ along the bar axis are also computed as follows:

$$M(x) = \int_{-d/2}^{d/2} \sigma_f(\phi(x),y).y.dA_s(y) \quad (13)$$

$$V(x) = \frac{dM(x)}{dx}. \quad (14)$$

Therefore, the shear force carried by reinforcing bars, so called 'dowel action', is directly calculated (Eq. (14)). The effect of shear stress due to bending curvature ($f_d(x) = V(x)/A_s$) on the yield stress of the bar (kinking of re-bars) can be taken into consideration by applying the Von Mises yield criterion and isotropic hardening rule as:

$$f'_y(x) = f_y\sqrt{1-3(f_d(x)/f_y)^2} \quad (15)$$

by which the reduced mean yield stress f'_y for checking the fiber stress of the bar is obtained.

Using the above iterative method, the phenomenon of reduction of the axial stiffness and strength of steel bar can be coherently explained. The reinforcing bar due to axial tensile stress and transverse shear displacement shows a gradual increase of plasticity both along the bar axis and across cross section close to crack surface. Even as the section at interface is in elastic state, the localization of plasticity can take place in the reinforcement inside concrete due to induced curvature. In this region, the mean stress profile is actually uniform; however the mean strain profile shows a significant non-uniformity due to induced curvature. Also, due to shear stress, the axial yield strength of fiber stress is reduced, and consequently the yielding of reinforcement is accelerated.

5. Bridging stress normal to cracks

When the crack is localized in the concrete domain, some residual tensile stresses are transferred across cracks due to interlocking of crack surfaces. As a result, the tensile stress at the crack plane does not drop to zero and concrete shows softening behavior after cracking. Actually, in reinforced concrete with an ordinary reinforcement ratio, the tension softening of concrete can be neglected compared to the bond stress transfer. However, in lightly reinforced concrete elements this phenomenon must not be neglected [16,17].

The tension-softening model is usually expressed as a relationship between crack width and bridging stress. Here Ushida's model [18] is adopted for analysis:

$$\sigma_{br} = f_t\left[1 + 0.5\omega\left(\frac{f_t}{G_f}\right)\right]^{-3} \quad (16)$$

where, σ_{br} is bridging stress transfer across the crack, f_t is tensile strength of concrete, ω is crack width and G_f is fracture energy of plain concrete.

6. Concrete in compression

The adopted analytical model here, for concrete under compression, is based on the elasto-plastic and fracture model (EPF) proposed by Maekawa and Okamura [19,20]. Prior to cracking, concrete is modeled as an elasto-plastic and fracture material and its mechanical behavior is identified as combined plasticity and continuum fracture. The biaxial stiffness and biaxial Poisson's ratios are formulated dependent on the loading conditions and strain-stress path [19,20]. After cracking, the strength and stiffness of concrete in the direction of the compressive stress are reduced compared to uncracked concrete [3,5,20]. The behavior of cracked concrete in compression with consideration to the influence of coexisting tensile strain is expressed as:

$$\begin{aligned} \sigma_2 &= -2k(e-e_p)f'_c \\ e &= \frac{\varepsilon_2}{\varepsilon_c} \\ k &= \zeta\exp\{-0.73e_{max}[1-\exp(-1.25e_{max})]\} \\ e_p &= e_{max}-\frac{20}{7}[1-\exp(-0.35e_{max})] \end{aligned} \quad (17)$$

where, σ_2 and ε_2 are compression stress and strain respectively, ε_c is strain corresponds to peak stress, e is normalized strain and e_{max} is maximum computed normalized strain in loading path, e_p and k are equivalent plastic strain and fracture parameter respectively. The reduction of compressive stiffness and strength after propagation of cracks in the model is mathematically considered by reduction factor ζ in the formulation of fracture parameter (Eq. (17)) as a function of strain perpendicular to the crack plane (ε_1):

$$\begin{aligned} &\zeta = 1.0, && \varepsilon_1 \le 0.0012 \\ &\zeta = 1-125(\varepsilon_1-0.0012), && 0.0012 < \varepsilon_1 < 0.0044 \\ &\zeta = 0.6, && \varepsilon_1 \ge 0.0044. \end{aligned} \quad (18)$$

7. Shear and dilatancy stresses transfer across cracks

Two main mechanisms of shear transfer along the crack plane are interaction between the rough surfaces of the crack and dowel action due to curvature of reinforcing bar at the crack section. As the shear displacement takes place at the crack interface, interlocking of aggregate particles with consequential tendency for widening of cracks (dilatancy) will occur. This crack widening increases the axial stress in reinforcing bar. At

the same time, shear displacement causes the flexural effect in reinforcing bar, which consequently produces the shear stress in some parts along the reinforcement close to crack interface, as detailed before.

The overall stress transfer system in reinforcing bar and concrete strictly controls the crack width and slip in RC member, which actually affects the shear transfer ability of crack plane. It is clear that the superposition of independent formulation of two different modes of stress transfer, which are dowel action and aggregate interlock, is different from the actual mechanism of shear transfer along the crack surface. Using the present analysis method, the dowel action and aggregate interlock can be treated in a unified concept, as the equilibrium of all forces mobilized in RC domain and compatibility conditions of displacement are satisfied in the analysis by considering the actual stiffness of all components.

The aggregate interlock model used here is based on the 'Universal Stress Transfer Model' proposed by Bujadham and Maekawa [21], which has large applicability and is verified by extensive experimental results under different monotonic and cyclic loading paths. The framework of the model is based on the original contact density model [22] with consideration to all characteristics of concrete stress transfer behavior e.g. microscopic friction on aggregate particles, anisotropic plasticity of contact stress and fracturing of contact units that control the path dependency of stress transfer across cracks. The model has been expressed and widely used elsewhere, which can be referred to for details [10,11,21]. For reinforced concrete with an ordinary reinforcement ratio, where several cracks can be developed in RC domain, the aggregate interlock model is simply formulated [22,23] as:

$$\tau_{agg} = 3.83 f_c^{1/3} \frac{\psi^2}{1+\psi^2} \tag{19}$$

$$\sigma_d = 3.83 f_c^{1/3} \left[\frac{\pi}{2} - \cot^{-1}\psi - \frac{\psi}{1+\psi^2} \right], \quad \psi = \frac{\delta}{\omega}, \text{ (Unit: MPa)} \tag{20}$$

where, τ_{agg} and σ_d are shear stress and dilatancy stress due to aggregate interlock, respectively. δ and ω are shear slip and crack opening, respectively.

8. Local analysis of RC membrane elements and averaging

In previous sections, the mechanism of stress transfer in RC membrane elements was analytically explained. Using the equilibrium and compatibility equations, the local analysis can be done on cracked RC elements. The local stresses of cracked concrete and reinforcing bars at crack surface have been shown in Fig. 10(a). These local stresses statically are equivalent with applied stresses. So, writing equilibrium equations in direction normal to cracks we have:

$$\sigma_d + \sigma_{br} = \sigma_X \cos^2\theta + 2\tau_{XY}\sin\theta\cos\theta + \sigma_Y \sin^2\theta - \rho_X \cdot f_{crX} \cdot \cos^2(\theta-\alpha) - \rho_Y \cdot f_{crY} \cdot \sin^2(\theta-\alpha) - f_{d\theta} \tag{21}$$

where, σ_d is dilatancy stress normal to cracks and σ_{br} is the bridging stress of cracked concrete, $f_{d\theta}$ is tensile stress induced by the shear stress in steel bars as follows:

$$f_{d\theta} = [\rho_{X'} f_{dX'} - \rho_{Y'} f_{dY'}] \sin(\theta-\alpha)\cos(\theta-\alpha) \tag{22}$$

where $f_{dX'}$ and $f_{dY'}$ are shear stresses of reinforcing bars at the crack location (dowel force in Eq. (14) divided by cross section area of bars) in X′ and Y′ direction, respectively. The shear stress in a steel bar is considered positive when its projection on the crack surface is in the positive direction of shear stress (τ_{12}) as shown in Fig. 10(a). Also, the equilibrium equation can be written based on the average stresses of concrete and reinforcements (Fig. 10(b)) as:

$$\sigma_1 = \sigma_X \cos^2\theta + 2\tau_{XY}\sin\theta\cos\theta + \sigma_Y \sin^2\theta - \rho_X \cdot \bar{f}_X \cdot \cos^2(\theta-\alpha) - \rho_Y \cdot \bar{f}_Y \cdot \sin^2(\theta-\alpha). \tag{23}$$

By comparison of the two above equations, total average tensile stress (tension stiffening) can be found as:

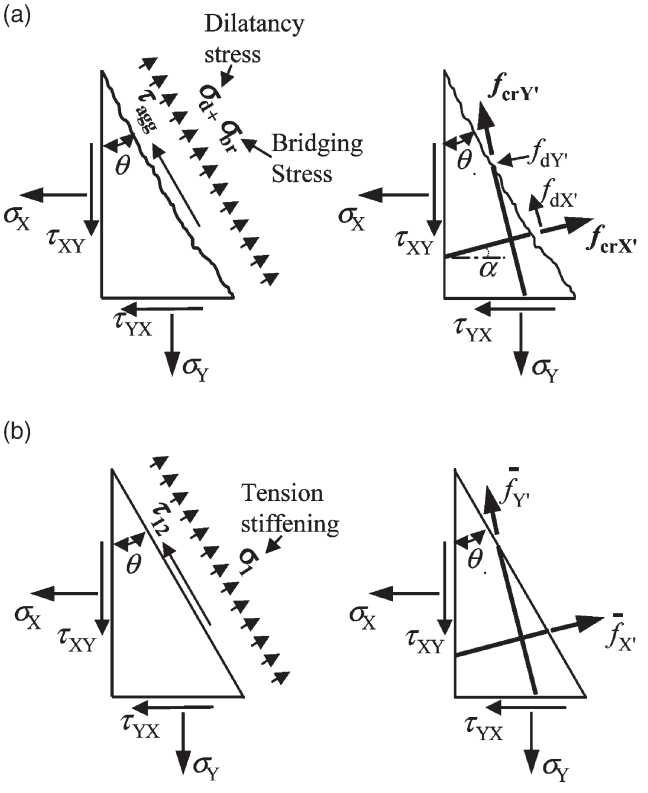

Fig. 10. Stress state of reinforcing bars and cracked concrete. (a) local stresses; (b) average stresses.

$$\sigma_1 = \rho_{X'}(f_{crX'} - \bar{f}_{X'})\cos^2(\theta-\alpha) + \rho_{Y'}(f_{crY'} - \bar{f}_{Y'})\sin^2(\theta-\alpha) + f_{d\theta} + \sigma_d + \sigma_{br} = \sigma_t + \sigma_d + \sigma_{br}. \quad (24)$$

Therefore, the tension stiffening of cracked concrete is expressed as the summation of tensile stress developed in concrete due to bond and shear stresses of steel bars (σ_t), bridging stress (σ_{br}), and dilatancy stress (σ_d). Eq. (24) shows the dependency of tension stiffening to crack and reinforcing bar inclination, reinforcement ratio (macro characteristics of RC elements), local characteristics of crack-reinforcing bars interaction (bond stress) and geometry of crack surface (aggregate interlock).

Using the equilibrium equations, the applied stress components can be expressed based on the stresses of cracked concrete and those of reinforcing bars. Replacing the local normal stress of concrete and also reinforcing bar stresses at crack plane by average tensile stress of concrete and reinforcing bar, the equilibrium equations can be expressed as:

$$\sigma_X = (\sigma_t + \sigma_d + \sigma_{br})\cos^2\theta + \sigma_2\sin^2\theta - 2\tau_{12}\sin\theta\cos\theta + \rho_{X'}\bar{f}_{X'}\cos^2\alpha + \rho_{Y'}\bar{f}_{Y'}\sin^2\alpha \quad (25)$$

$$\sigma_Y = (\sigma_t + \sigma_d + \sigma_{br})\sin^2\theta + \sigma_2\cos^2\theta + 2\tau_{12}\sin\theta\cos\theta + \rho_{X'}\bar{f}_{X'}\sin^2\alpha + \rho_{Y'}\bar{f}_{Y'}\cos^2\alpha \quad (26)$$

$$\tau_{XY} = (\sigma_t + \sigma_d + \sigma_{br} - \sigma_2)\sin\theta\cos\theta + \tau_{12}(\cos^2\theta - \sin^2\theta) + (\rho_{X'}\bar{f}_{X'} - \rho_{Y'}\bar{f}_{Y'})\sin\alpha\cos\alpha \quad (27)$$

where, σ_X, σ_Y are the applied normal stresses in X and Y directions respectively, and τ_{XY} is the applied shear stress in X–Y direction. Sign convention is considered, as shown in Fig. 2.

Using strain compatibility relationship, the strains in global direction (X–Y coordinate system) can be expressed in terms of three components of strain (ε_1, ε_2, γ_{12}) in local axes of cracked concrete:

$$\varepsilon_X = \varepsilon_1\cos^2\theta + \varepsilon_2\sin^2\theta - \gamma_{12}\sin\theta\cos\theta \quad (28)$$

$$\varepsilon_Y = \varepsilon_1\sin^2\theta + \varepsilon_2\cos^2\theta + \gamma_{12}\sin\theta\cos\theta \quad (29)$$

$$\gamma_{XY} = 2(\varepsilon_1 - \varepsilon_2)\sin\theta\cos\theta + \gamma_{12}(\cos^2\theta - \sin^2\theta). \quad (30)$$

Also, the average strain of reinforcing bars in local coordinate system can be expressed as:

$$\varepsilon_{X'} = \varepsilon_1\cos^2(\theta-\alpha) + \varepsilon_2\sin^2(\theta-\alpha) - \gamma_{12}\sin(\theta-\alpha)\cos(\theta-\alpha) \quad (31)$$

$$\varepsilon_{Y'} = \varepsilon_1\sin^2(\theta-\alpha) + \varepsilon_2\cos^2(\theta-\alpha) + \gamma_{12}\sin(\theta-\alpha)\cos(\theta-\alpha) \quad (32)$$

$$\gamma_{X'Y'} = 2(\varepsilon_1 - \varepsilon_2)\sin(\theta-\alpha)\cos(\theta-\alpha) + \gamma_{12}(\cos^2(\theta-\alpha) - \sin^2(\theta-\alpha)). \quad (33)$$

Using the compatibility equations (Eqs. (28)–(33)) and considering the average strain of concrete in the local coordinate system (ε_1, ε_2 and γ_{12}) as the primary unknown parameters, the average steel strains, and also global strains of RC elements, can be obtained.

Fig. 11 shows the state of stresses between two adjacent cracks. Using the governing equations of stress transfer along the steel bar, for any given average steel strains, the profile of strains and stresses along the reinforcing bar and its local stress at crack surface, and also the average stress, are computed as shown in Fig. 9. The lengths of reinforcing bars are obtained based on the crack spacing and angle between reinforcing bar and crack direction as:

$$L_{eX'} = \frac{S_{XY}}{\cos(\theta-\alpha)} \quad (34)$$

$$L_{eY'} = \frac{S_{XY}}{\sin(\theta-\alpha)} \quad (35)$$

where, $L_{eX'}$ and $L_{eY'}$ are the length of reinforcing bar between two adjacent cracks, S_{XY} is crack spacing that is initially considered equal to length of specimen in the direction of principle tensile stress. Average crack width (ω) and shear slip (δ) are obtained by multiplication of tensile strain and shear strain of cracked concrete by crack spacing:

$$\omega = \varepsilon_1 \times S_{XY} \quad (36)$$

$$\delta = \gamma_{12} \times S_{XY}. \quad (37)$$

The elastic deformations of concrete between two adjacent cracks are neglected, as they are very minor compared to crack opening and sliding. Therefore, in each loading step, the crack width and slip and consequently the local stress of cracked concrete (bridging stress, shear and dilatancy stress), can be computed as described before (Eqs. (16), (17), (19), (20) and (24)).

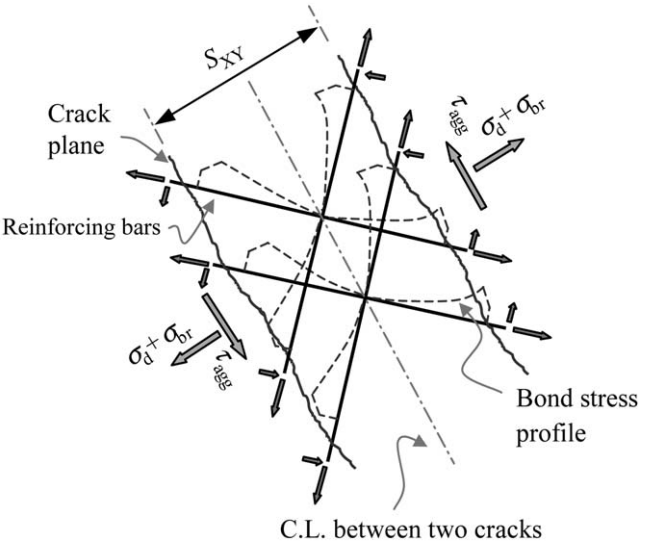

Fig. 11. The state of stress between two adjacent cracks.

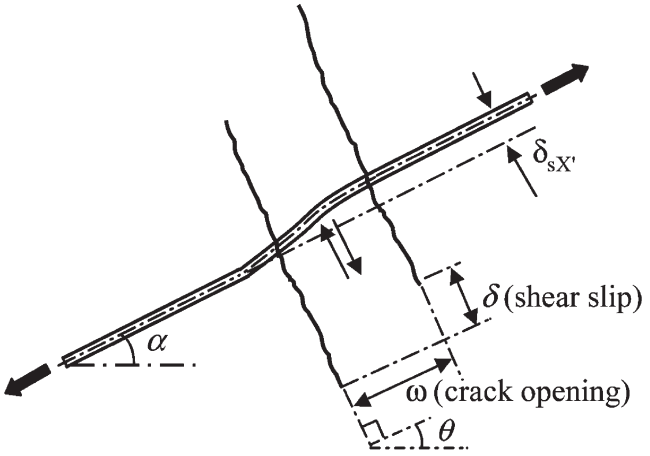

Fig. 12. Curvature of reinforcing bar due to opening and sliding.

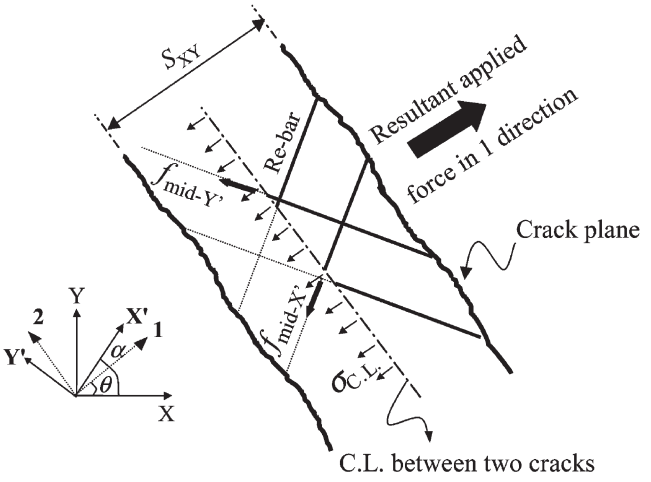

Fig. 13. Local tensile stress on centerline of two adjacent cracks.

Satisfying the displacement compatibility at the crack plane, the deflection of reinforcing bar at interface (kinking of reinforcements) is obtained as (Fig. 12):

$$\delta_{sX'} = \omega\sin(\theta-\alpha) + \delta\cos(\theta-\alpha) \quad (38)$$

$$\delta_{sY'} = \omega\cos(\theta-\alpha) - \delta\sin(\theta-\alpha) \quad (39)$$

where, $\delta_{sX'}$ and $\delta_{sY'}$ are the deflections of reinforcing bars in X′ and Y′ direction at the crack location, respectively.

Considering the curvature shape of reinforcements close to crack surface, the bending moment and shear stresses (dowel action) in the curvature zone are computed as explained before. The total shear stress that can be transferred across cracks will be the summation of stress transfer by concrete and reinforcing bars in X′ and Y′ directions as:

$$\tau_{12} = \tau_{st} + \tau_{agg} \quad (40)$$

$$\tau_{st} = \rho_{X'} f_{dX'} \cos^2(\theta-\alpha) + \rho_{Y'} f_{dY'} \sin^2(\theta-\alpha) - [\rho_{X'}(f_{crX'} - \bar{f}_{X'}) - \rho_{Y'}(f_{crY'} - \bar{f}_{Y'})]\sin(\theta-\alpha)\cos(\theta-\alpha). \quad (41)$$

In each step, the local tensile stress of concrete between two adjacent cracks can be calculated by satisfying the equilibrium conditions at centerline between cracks:

$$\sigma_{C.L.} = \text{resultant stress normal to C.L.} - [\rho_{X'} f_{mid-X'} \cos^2(\theta-\alpha) + \rho_{Y'} f_{mid-Y'} \sin^2(\theta-\alpha)] \quad (42)$$

where, $f_{mid\text{-}X'}$ and $f_{mid\text{-}Y'}$ are the steel stresses between two adjacent cracks (Fig. 13). When the maximum local

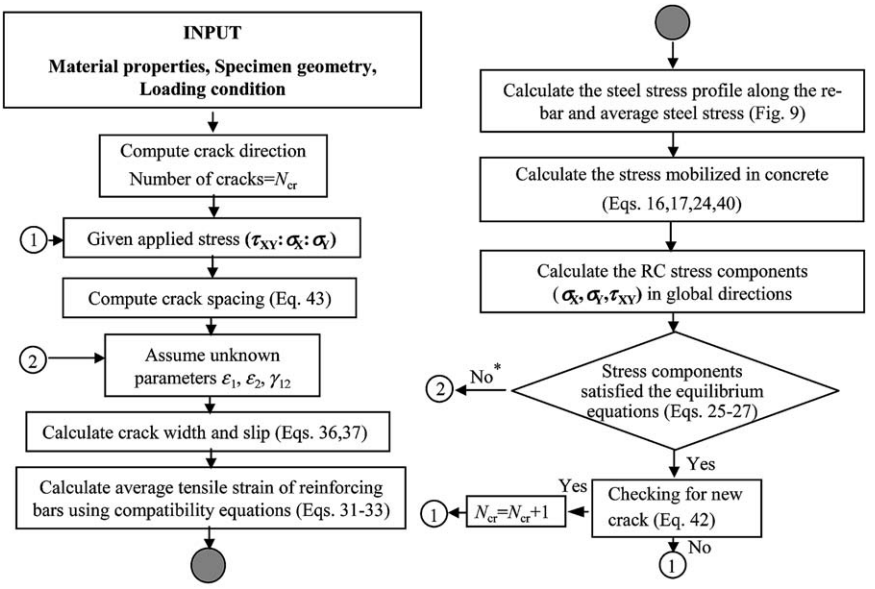

* Note: The system of equations involving 3 equations (equilibrium equations) with 3 unknown parameters (concrete strains) is solved using an iterative method.

Fig. 14. Flowchart of computation.

Table 1
Specimen details and loading conditions

Panel	Concrete f'_c (MPa)	ε_c $\times 10^{-3}$	Reinforcing bars ρ_X %	f_{yX} (MPa)	d_X (mm)	ρ_Y %	f_{yY} (MPa)	d_Y (mm)	α Deg	Loading τ_{XY}:σ_X:σ_Y	Experiment by
PC1A	27.9	−1.85	1.65	500	5.72	0.825	500	5.72	0	1:0:0	Vecchio and Chan [24]
PC4	24.9	−1.70	1.65	260	5.72	0.825	260	5.72	0	1:−0.39:−0.39	
PC7	28.7	−1.85	1.65	390	5.72	0.825	390	5.72	0	1:0.32:0.32	
A2	41.2	−2.10	1.193	463	15	1.193	463	15	45	0:1.0:−1.0	Pang and Hsu [5]
A3	41.6	−1.94	1.789	447	20	1.789	447	20	45	0:1.0:−1.0	
B1	45.3	−2.15	1.193	463	15	0.596	445	10	45	0:1.0:−1.0	
B2	44.1	−2.35	1.789	447	20	1.193	463	15	45	0:1.0:−1.0	

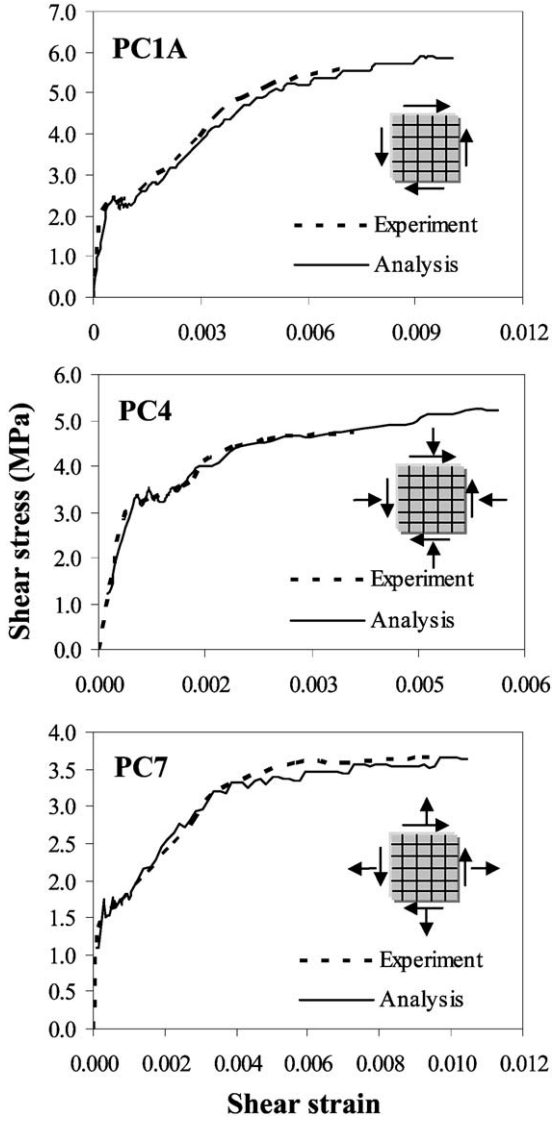

Fig. 15. Comparison with experiments results (PC1A, PC4, PC7) by Vecchio and Chan [24].

concrete stress exceeds the tensile strength of concrete, a new crack in the middle of initial cracks is introduced and computation is carried out with new crack spacing. However, it should be noted that because of non-uniformity of concrete the location of new cracking is not necessarily in the middle of two previous cracks, so the calculated crack spacing could be assumed as average crack spacing.

The procedure is followed until cracks reach a stabilized state which takes place either after yielding of reinforcing bars or when the crack spacing becomes so small that the bond stress transfer to concrete is not sufficient enough for any further cracking. Since, in reality, it is not possible for two cracks to initiate simultaneously, as experimentally shown by Goto [9], Rizkalla and Hwang [25], in each cracking state it is assumed that just one new crack generates in RC domain, and the average crack spacing is computed as:

$$S_{XY} = \frac{S_0}{N_{cr}} \tag{43}$$

where, S_0 is initial crack spacing (length of specimen normal to crack direction) and N_{cr} is number of generated cracks.

It was assumed in this work that the direction of cracks remain fixed during loading. In fact, large anisotropy of steel forces at crack location sometimes results in rotation of crack from its initial orientation [3]. This phenomenon, which depends on the loading condition and reinforcement ratio, can also be investigated through the local load transfer mechanism in RC domain, however it is not discussed in this work.

9. Computation procedure

Using the compatibility equations (Eqs. (28)–(33)) and considering the average strains of cracked concrete as the primary unknown parameters, the average steel strains in its local coordinate systems are obtained. Consequently, by local analysis, the entire stress transfer

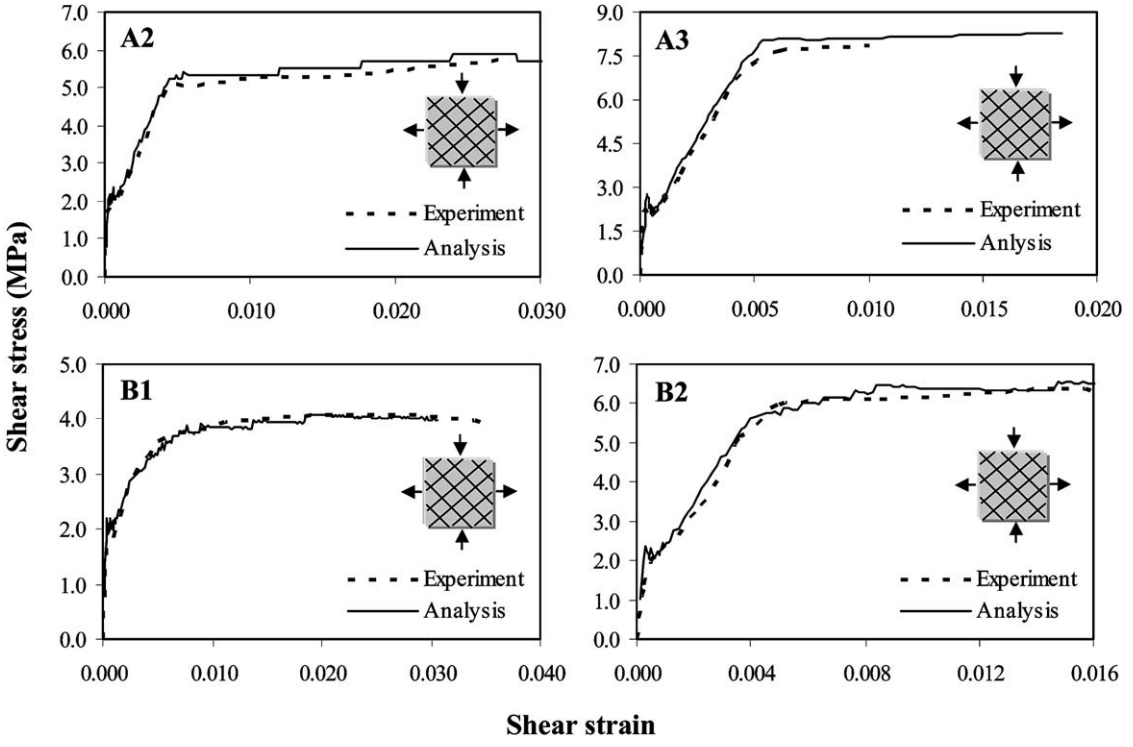

Fig. 16. Comparison with experimental results (A2, A3, B1, B2) by Pang and Hsu [5].

in RC domain through both reinforcing bars and cracked concrete, in other words all quantities in right hand sides of equilibrium equations (Eqs. (25)–(27)), are obtained as explained before. Therefore, for any given applied stress, the unknown average strains can be determined in an iterative way (using an iterative solution method such as Newton-Raphson method) as flowchart shown in Fig. 14.

10. Verification of the model

To verify the reliability of the proposed analytical method, a comparison with experimental work conducted by other researchers is carried out. The series of experimental results involving reinforced concrete panel specimens subjected to in-plane force conducted at the University of Toronto by Vecchio and Chan [24] and at the University of Houston by Pang and Hsu [5] were selected. The details of the specimens and loading conditions are listed in Table 1.

All specimens have been orthogonally reinforced by deformed steel bars. In the analysis, the tensile strength of concrete was considered based on the reported cracking load that is less than the tensile strength of concrete based on the splitting test on cylindrical specimens. The comparison between experiment and analytical results, in terms of shear stress-strain relationship, are illustrated in Figs. 15 and 16. Using the proposed method, the spatial average stress-strain relationship of reinforcing bars and cracked concrete, and at the same time average crack spacing and crack width are computed in an acceptable way, close to reality of stress transfer in RC domain. The comparison between computed average stress-strain relationships of reinforcing bars for panel A2 and A3 with experimental results of panels tested by Pang and Hsu [5] are shown in Fig. 17. It should be noted that the measured average stress-strain relationship of reinforcing bar in the experiment is valid until yielding of reinforcing bars. However, the post yield behavior can be checked through the overall behavior of the panels (Fig. 16). Generally, good agreement between the experimental results and local analysis is found.

As in the proposed method, all stress components mobilized in RC domain are obtained in terms of local stress-strain characteristics and local response of components, the average tensile stress-strain relationship of reinforcing bars considering crack direction and kinking effect at crack location, and also average tensile stress-strain relationship of cracked concrete, that is, the summation of tensile stress transfer due to bond, bridging stress and dilatancy stress and the participation of each factor in the response of membrane element, can be investigated.

As an example, the computed average tensile stress-strain relationship for panels A2 and B1 are shown in Fig. 18. Panel A2 is a sample of RC elements with symmetric geometry and loading condition. In such a case, no shear slip takes place on the crack surface (no dilatancy stress); as a result, the tension stiffening is the sum-

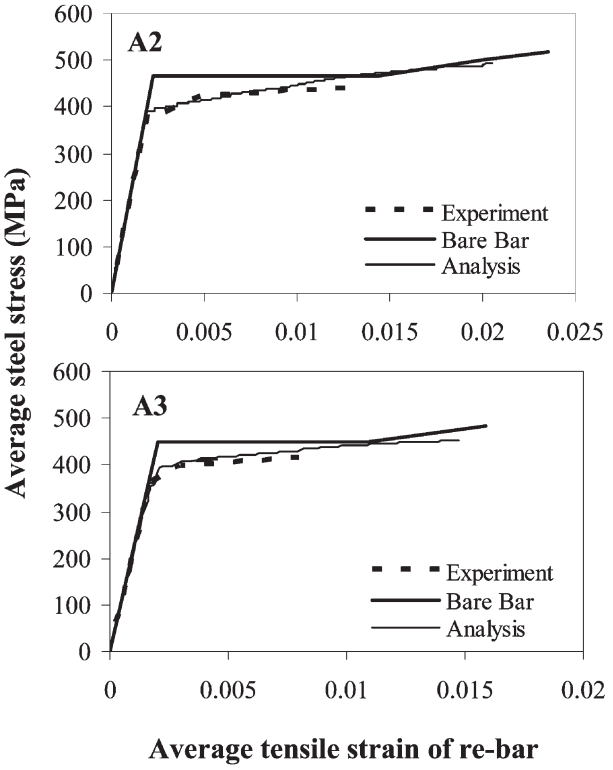

Fig. 17. Comparison between computed average stress-strain relationship of re-bars with experimental results (A2, A3) by Pang and Hsu [5].

mation of the tensile stress transfer due to bond and bridging stress. It is shown that the contribution of bridging stress in tension stiffening for such a case with adequate reinforcement ratio (not low reinforcement ratio) is ignorable compared to bond stress. In panel B1, due to anisotropy of reinforcing bars at the crack surface, considerable dilatancy stress due to aggregate interlock takes place as a compression force normal to the crack surface which increases as the shear slip at cracked section increases.

11. Conclusions

The rational, accurate and versatile consideration of macroscopic stress transfer ability of cracked RC element in numerical modeling is substantial for the accurate prediction of cracking response, strength, deformational behavior and failure mode of RC structures. After review of some analytical models for local stress transfer in RC domain, the frame of the new methodology was described for crack analysis of RC membrane elements subjected to in plane stresses. Crack spacing, crack width and slip, average stress-strain relationship of reinforcing bars and concrete are determined from the equilibrium of local and applied stresses and compatibility conditions of displacement at crack location. The result of the analysis can be considered as a basis of the enhanced smeared crack approach as the stiffness modules of all components are developed based on the local characteristics of each component. Through a parametric study, the influence of reinforcement ratio and arrangement, bar diameter, crack inclination, element size (size effect) and material properties on the post cracking constitutive laws of concrete and reinforcement can be investigated for development of rational constitutive models. Such a constitutive relationship is necessary for finite element analysis of many RC structures treated as assembling of RC membrane elements.

The contribution of reinforcements on shear transfer across cracks (dowel action) and also the kinking effect of reinforcing bars can be considered in the analysis in a satisfactory manner. The crack spacing and crack width strictly depends on bond performance between concrete and reinforcing bars, so considering the real bond characteristics between concrete and reinforcing bars, the crack propagation in the RC domain can be investigated through the proposed method. Regarding the proposed methodology, further research concerning bond performance is proposed.

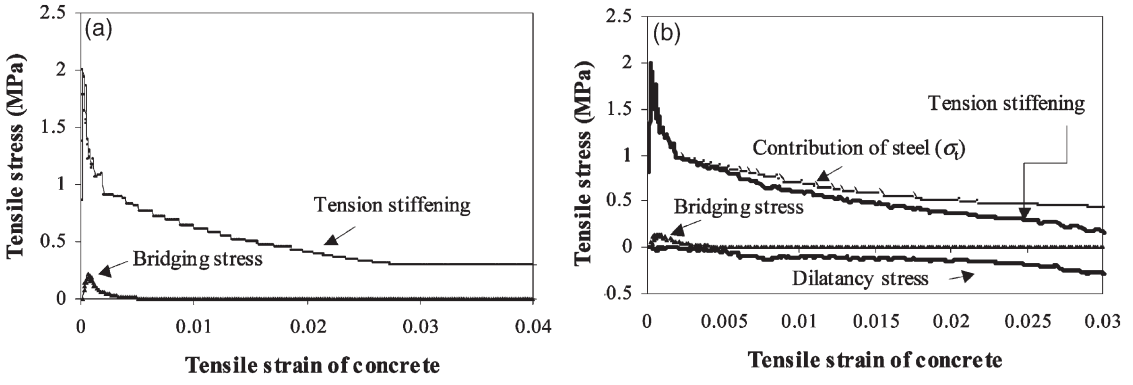

Fig. 18. The computed tensile stress components mobilized in RC domain. (a) panel A2; (b) panel B1.

References

[1] Hsu TTC. Nonlinear analysis of concrete membrane elements. ACI Structural Journal 1991;88(5):552–61.

[2] Izumo J, Shima H, Okamura H. Analytical model for RC panel elements subjected to in-plane forces. Concrete Library of JSCE 1989;12:155–81.

[3] Vecchio FJ, Collins MP. The response of reinforced concrete to in-plane shear and normal stresses. Publication No. 82-03, University of Toronto, 1982.

[4] Hauke B, Maekawa K. Three-dimensional modeling of reinforced concrete with multi-directional cracking. Journal of materials, Conc. Struct., Pavement, JSCE 1999;45(634):349–68.

[5] Pang X, Hsu TTC. Behavior of reinforced concrete membrane elements in shear. ACI Structural Journal 1995;92(6):665–79.

[6] Belletti B, Cerioni R, Iori I. Physical approach for reinforced-concrete (PARC) membrane elements. Journal of Structural Engineering 2001;127(12):1412–26.

[7] Kaufmann W, Marti P. Structural concrete: cracked membrane model. Journal of Structural Engineering 1998;24(12):1467–75.

[8] Shima H, Chou L, Okamura H. Micro and macro models for bond in reinforced concrete. Journal of faculty of engineering, The University of Tokyo (B) 1987;39(2):133–94.

[9] Goto Y. Cracks formed in concrete around deformed tension bars. ACI Journal 1971;68(4):244–51.

[10] Qureshi J. Modeling of stress transfer across reinforced concrete interfaces. Doctoral dissertation, Department of Civil Engineering, The University of Tokyo, 1993.

[11] Qureshi J, Maekawa K. Computational model for steel embedded in concrete under combined axial pullout and transverse shear displacement. Proceedings of JCI 1993;15(2):1249–54.

[12] Shin H. Finite element analysis of reinforced concrete members subjected to reversed cyclic in-plane loadings. Doctoral dissertation, Department of Civil Engineering, The University of Tokyo, 1988.

[13] Dei Poli S, Di Prisco M, Gambarova PG. Shear response, deformation and subgrade stiffness of a dowel bar embedded in concrete. ACI Structural Journal 1992;89(6):665–75.

[14] Dulacska H. Dowel action of reinforcement crossing cracks in concrete. ACI Journal 1972;69(12):754–7.

[15] Mishima T, Maekawa K. Development of RC discrete crack model under reversed cyclic loads and verification of its applicable range. Concrete Library of JSCE 1992;20:115–41.

[16] Fantilli AP, Ferretti D, Iori I, Vallini P. Behavior of R/C elements in bending and tension: The problem of minimum reinforcement ratio. In: Carpiniteri A, editor. Minimum reinforcement in concrete members. ESIS Publication, 24. Torino, Italy: ESIS; 1991. p. 99–125.

[17] Salem H. Enhanced tension stiffening model and application to nonlinear dynamic analysis of reinforced concrete. Doctoral dissertation, Department of Civil Engineering, The University of Tokyo; 1998.

[18] Ushida Y, Rokugo K, Koyanagi W. Determination of tension softening diagrams of concrete by means of bending tests. Proceedings of JSCE 1991;14(426):203–12.

[19] Maekawa K, Okamura H. The deformational behavior and constitutive equation of concrete using the elasto–plastic and fracture model. Journal of Faculty of Engineering, The University of Tokyo (B) 1983;37(2):253–328.

[20] Okamura H, Maekawa K. Nonlinear analysis and constitutive models of reinforced concrete. Tokyo, Japan: Gihodo-Shuppan, 1991.

[21] Bujadham B, Maekawa K. The universal model for stress transfer across cracks in concrete. Proc of JSCE 1992;17(451):277–87.

[22] Li B, Maekawa K, Okamura H. Contact density model for stress transfer across cracks in concrete. Journal of the Faculty of Engineering, University of Tokyo (B) 1989;40(1):9–52.

[23] Soltani M. Micro computational approach to post cracking constitutive laws of reinforced concrete and application to nonlinear finite element analysis. Doctoral dissertation, Department of Civil Engineering, The University of Tokyo, 2002.

[24] Vecchio FJ, Chan CCL. Reinforced concrete membrane elements with perforations. Journal of Structural Engineering 1990;116(9):2344–60.

[25] Rizkalla S, Hwang L. Crack prediction for members in uniaxial tension. ACI Journal 1984;81(44):572–9.